University of Texas Rio Grande Valley

ScholarWorks @ UTRGV

Chemistry Faculty Publications and Presentations

College of Sciences

11-20-2019

Novel silica filled deep eutectic solvent based nanofluids for energy transportation

Changhui Liu
China University of Mining Technology - Xuzhou

Hui Fang
China University of Mining Technology - Xuzhou

Xinjian Liu
China University of Mining Technology - Xuzhou

Ben Xu
The University of Texas Rio Grande Valley, ben.xu@utrgv.edu

Zhonghao Rao
China University of Mining Technology - Xuzhou

Follow this and additional works at: https://scholarworks.utrgv.edu/chem_fac

Part of the Chemistry Commons, and the Nanoscience and Nanotechnology Commons

Recommended Citation

Liu, C., Fang, H., Liu, X., Xu, B., & Rao, Z. (2019). Novel Silica Filled Deep Eutectic Solvent Based Nanofluids for Energy Transportation. ACS Sustainable Chemistry & Engineering, 7(24), 20159–20169. https://doi.org/10.1021/acssuschemeng.9b06179

This Article is brought to you for free and open access by the College of Sciences at ScholarWorks @ UTRGV. It has been accepted for inclusion in Chemistry Faculty Publications and Presentations by an authorized administrator of ScholarWorks @ UTRGV. For more information, please contact justin.white@utrgv.edu, william.flores01@utrgv.edu.

Novel silica filled deep eutectic solvent based nanofluids for energy transportation

Changhui Liu,[a,b] Hui Fang,[a,b] Xinjian Liu,[a,b] Ben Xu,[c] and Zhonghao Rao*[a,b]

[a] Jiangsu Province Engineering Laboratory of High Efficient Energy Storage Technology and Equipments, China University of Mining and Technology, No. 1, Daxue Road, Xuzhou 221116, China.

[b] Laboratory of Energy Storage and Heat Transfer, School of Electrical and Power Engineering, China University of Mining and Technology, No. 1, Daxue Road, Xuzhou, 221116, China.

[c] Department of Mechanical Engineering, University of Texas Rio Grande Valley, 1201 West University Dr., Edinburg, Texas 78539-2909, USA.

Changhui Liu:

Email: liuch915@cumt.edu.cn; TEL:86-516-83592000.

Hui Fang:

Email: fanghui@cumt.edu.cn; TEL:86-516-83592000.

Xinjian Liu:

Email: liuxinjian@cumt.edu.cn; TEL:86-516-83592000.

Ben Xu

Email: ben.xu@utrgv.edu; TEL: 956-665-2896.

*Corresponding author:

Zhonghao Rao:

Email: raozhonghao@cumt.edu.cn; TEL: 86-516-83592000.

Novel silica filled deep eutectic solvent based nanofluids for energy transportation

Changhui Liu,[a,b] Hui Fang,[a,b] Xinjian Liu,[a,b] Ben Xu,[c] and Zhonghao Rao*[a,b]

[a] Jiangsu Province Engineering Laboratory of High Efficient Energy Storage Technology and Equipments, China University of Mining and Technology, Xuzhou 221116, China. Email: raozhonghao@cumt.edu.cn.

[b] Laboratory of Energy Storage and Heat Transfer, School of Electrical and Power Engineering, China University of Mining and Technology, Xuzhou, 221116, China.

[c] Department of Mechanical Engineering, University of Texas Rio Grande Valley, Edinburg, TX 78539, USA.

Abstract: Liquid range of nanofluids is a crucial parameter as it intensively determines their application temperature scope. Meanwhile, improved thermal conductivity and stability are of great significances and comprise the main fundamental research topics of nanofluids. In this work, 2-butoxy-3,4-dihydropyran (DP), produced from a convenient one-pot three-component reaction in water, was employed as dual lipophilic brusher and metal nanoparticle anchor. It was found that DP was able to enhance the dispersing ability and thermal conductivity of SiO_2 nanoparticle filled deep eutectic solvent (DES) based nanofluids simultaneously. The key to the success of this protocol mainly relies on the electrophilic property and acetylacetonate moiety of DP, which ensures the formation of DP surficial modified and copper nanoparticle coated silica. Molecular dynamics simulation revealed that the hydrogen bonding effect between base solvent and alkane chain of nanoparticle was responsible for the enhanced affinity, which thus resulted in an improved stability. Viscosities of the nanofluids dropped within a certain range owing to the ruin of hydrogen bonding association among solvent molecules resulted by the hydrogen bonding effect between nanoparticle and solvent. Thermal conductivity of the copper modified silica filled DES nanofluids exhibits a maximum 13.6% enhancement, which demonstrated the advantages of this chemical covalent protocol. Additionally, study upon viscosity and convective heat transfer coefficient of the nanofluids with varies types of silica nanoparticle and DES base solvents indicated that a 24.9% heat transfer coefficient enhancement was gained that further revealed the superiority of this protocol.

Key words: Nanofluids; chemical modified silica; deep eutectic solvents; energy transportation.

Introduction

Nanoscale materials and devices hold great potential for improved energy conservation, conversion, or harvesting. Heat transfer fluids, also known as working fluids, have a crucial role in thermal transport applications.[1-3] However, traditionally used working fluids, such as water, mineral oil or organic alcohol were heavily limited by their relatively poor thermal conductive performance.[4] In particular, with the rapid advances of electrical setup and continuous shrinkage of mechanic facilities, highly efficient heat removal has been becoming an urgent demand.[5-7] Nanofluid, which was first termed by Choi, mainly constituted by a nanofiller and a base solvent, was a good solution to the poor thermal conductivity of single phase working fluid.[8-10] Base solvent has a vital role in nanofluids since it determines the main thermophysical properties, eg. thermal conductivity, dragging coefficient, boiling point and melting point, etc. Moreover, it is the place for reserving nanoparticle, it highly impacts the dispersing ability and stability of the nanofluid system. Traditionally used base solvent can be generally classified into water, mineral oil and organic alcohol.[11, 12] As evidenced on their common inherent physical properties, they are quite limited by their relatively short liquid range, which will become invalid under complex temperature conditions or specific device requirements. Ionic liquid, emerging as a new base solvent alternative, has been gaining continuous interest due to less volatile, high boiling point and chemical stability. While, ionic liquid usually suffers from high cost, tedious preparation process and environmental issues.[13-15] Meanwhile, high temperature molten salt is another widely adopted base solvent system mainly works for the field of high temperature solar collector.[16] However, the high melting point of the salt is the main obstacle as it will inevitably cause the clogging of the flow system at a low temperature. Therefore, exploring a new base solvent system that could fulfil both wide liquid range and environmental benign requirement is an urgent topic that needs to be deeply studied.

Deep eutectic solvent (DES), which is mainly constituted by two or three simple chemicals through intermolecular hydrogen bonding effect, has attracted ample attention owing to its similar properties with traditionally used ionic liquids.[17-20] DES has been proven to possess high boiling point and less volatile. In addition, it contains vast, nonsymmetric ions that have low lattice energy and thus low melting points. Notably, compared with ionic liquid, it is much less costly and environmental friendly. So far, it has been widely adopted in catalysis, electrochemistry, material

chemistry and so on.[20, 21] The research for its application as a working fluid and a base solvent of nanofluids for heat transportation has also been initiated.[22-26] Despite its superior thermophysical properties in terms of wide liquid range and accessibility, the stability issue of its based nanofluid is another problem that restricts its development. Adding a dispersant is a wide recognized protocol to address dispersing problem as it can inhibit the aggregation of nanoparticle. Whereas, it seems to be ineffective towards the DES base solvent system since the existence of dispersant, which usually composed by a cation and anion, will undoubtedly cause the interference of hydrogen bonding between the hydrogen donor and acceptor components and lead to the complexity of the whole solvent system.[27, 28] On the other hand, aging of dispersant would lead an irreversible damage of working efficiency of nanofluids during a long-term using.[29, 30] Decomposition of dispersant in some extreme condition, such as high temperature, would accelerate the failure process of the nanofluid. Further, the existence of dispersant in nanofluids also brings some negative influence to the performance of nanofluids, for instance, viscosity increase and thermal conductivity reduction.[31] Therefore, so far, a DES based nanofluid should face the problem of the absence of a dispersant. To alleviate this problem, a nanoparticle that has a good affinity with DES, such as coordination or hydrogen bonding effect, was recommended. However, this effect also brings some negative aspects to the behaviour of nanofluids, for example, our previous work revealed that the addition of Al_2O_3 nanoparticle resulted in a decreasing of thermal conductivity of glycerol/chlorine DES nanofluids owing to the motion activity declining of glycerol molecule caused by the hydrogen bonding association with Al_2O_3.[32]

Covalently installing an organic chain on the surface of nanoparticle is an efficient way to improve the stability of nanofluids in particular for organic solvent based nanofluids owing to the affinity enhancement between nanoparticle and base solvent. Some relevant research can be found in literatures, for example, Lukehart et al. demonstrated the deaggregation of an oxidized ultradispersed diamond in dimethylsulfoxide (DMSO) followed by reacting with glycidol monomer to produce a covalent surface modified nanodiamond filled ethylene glycol (EG) based nanofluid.[33] The research results indicated that the covalent nanodiamond modification gave a 2-fold greater thermal conductivity than that of hydrogen-bonding interaction modification strategy at the similar concentration. Zhang et al. synthesized a graphene which possessed a similar molecular chain with

ionic liquid [HMIM]BF_4, it was verified that the dispersion stability was greatly enhanced owing to the covalent modification.[34] The photo conversion performance of nanofluids was also enhanced as a consequence of the promising stability. Previously, we developed Lewis acid catalysis induced ring-opening reactions of 2-butoxy-3,4-dihydropyran (DP) with various of nucleophiles, among them, mercaptans quite stood out that it was able to react with DP with high regio-selectivity and yields.[35-40] Inspired by this reaction, we envision that DP deemed to be able to link onto the surface of SH containing silica with the aid of a Lewis acid. Moreover, owing to the coordination effect of acetylacetonate moiety in DP molecule, copper can be anchored on the surface of this modified silica with the purpose of thermal conductivity enhancement.

In this paper, in order to find a high thermal conductivity and stable DES based nanofluid system to address the short liquid range of traditional base solvent system based nanofluids (**Fig. 1**), a covalent modification and metal hybrid protocol on silica nanoparticle was investigated. SH containing silica nanoparticle was synthesized from TEOS and MPTMS through a sol-gel reaction with the aid of catalytic amount of *n*-hexadecylamine. The synthesized silica was subjected to react with DP under the catalysis of Lewis acid $ZnCl_2$. The copper nanoparticle was evenly coated on the surface of silica thanks to the anchoring effect derived from the acetylacetonate group on the surface of silica moiety. The stability improvement mechanism behind was revealed by using molecular dynamic simulation approach. Nanofluids prepared from DP modified silica and DES were studied comprehensively regarding their stability and thermo-physical properties.

Results and discussion

Our study commenced from the synthesis of DP derivative. 1-(Vinyloxy)butane, aqueous formaldehyde and acetylacetone were mixed and allowed to stir at 80 ^oC for 6 hours to complete the reaction in almost quantitative yields which were in good accordance with the results reported by Gu et al.[41] SH containing silica, SiO_2-SH, synthesized from TEOS and MPTMS, some reaction parameters, including catalyst, solvent and reaction temperature etc., were applied to explore a uniform size distributed nanoparticle. After a careful study upon the synthetic parameters, the optimized reaction condition was determined to be 17.6 mol% of *n*-hexadecylamine as catalyst, H_2O/EtOH 18/35 (*V*/*V*) as solvent, reacted at 50 ^oC for 20 h. DP decorated silica, which was named as SiO_2-SH-DP, was then prepared by treating SiO_2-SH with excess amount of DP under the

catalysis of 20 mol% of $ZnCl_2$. The final copper coated silica nanoparticle, SiO_2-SH-DP-Cu, was obtained by treating SiO_2-SH-DP with $Cu(acac)_2$ and $NaBH_4$ sequentially (**Fig. 2**). To facilitate reading and understanding, the name of different silica nanoparticle was listed and explained in table 1. After synthesis of the chemical modified silica nanoparticle, some analyses with respect to the above mentioned three different kinds of materials were conducted. As shown in **Fig. 3a-c**, SEM images show that the morphology of the as-prepared chemical modified silica displays a uniform size distribution with a sphere like shape. TEM images (**Fig. 3d-e)** further proved that the morphology of the obtained materials is a uniform sphere structure with an average diameter of around 300 nm. It should be mentioned that the surface of the prepared SiO_2-SH material is quite smooth without observation of nanoporous structure. The morphology of DP modified SiO_2-SH shows no significant change after fixing with organic linker that neither nanoparticle aggregation nor broken of the nanoparticle is observed from the TEM image (**Fig. 3h)**. What'more, the surface of the silica nanoparticle is seemly smoother than that of SiO_2-SH owing to the existence of the organic chain derived from DP. Interestingly, the surface of the silica becomes rough after coating with Cu nanoparticle as evidenced in **Fig. 3i**, which clearly demonstrates the existence of Cu on the surface of DP modified silica. Meanwhile, diameter of the SiO_2-SH-DP-Cu increases a little bit due to the contribution of Cu layer. Moreover, there is no observation of nanoparticle destruction or aggregation after a blending with copper acetate and reduction treatment. Moreover, EDS mapping further evidences that Cu and other elements were uniformly distributed on the surface of SiO_2-SH-DP-Cu (**Fig. 3j**).

XRD spectra of the above mentioned three different types of silica samples were tested. As shown in **Fig. 4a**, all of the silica samples display a typical SiO_2 peak appeared at $2\theta=22.5^o$, which illustrates the main component of the sample is still SiO_2. While, we did not find the response of copper from the spectra of SiO_2-SH-DP-Cu, probably due to the relatively low concentration of Cu in the sample. FT-IR spectra of the prepared samples in **Fig. 4b** proves the successful covalently bonding of DP on the surface of SiO_2-SH since the observation of peak in 1750 cm^{-1}, which is attributed to the carbonyl group of ring-opening structure of DP. The adsorption peak in the range of 1700-1750 cm^{-1} becomes boarder when loaded Cu on the surface of SiO_2-SH-DP, which reveals the coordination effect of Cu on carbonyl group, and this phenomenon is quite in agreement with the

literature result.[42] ^{13}C MAS NMR was also conducted to prove the covalent bond formation between SiO_2 and DP. As shown in **Fig. 4c**, the appearance of peak at 203.1 ppm is assigned to the carbonyl group of SiO_2-SH-DP, accompanied by the appearance of a characteristic band of a carbonyl group at 1700 cm^{-1} in FT-IR spectra, constitute a strong evidence of the nondestructive tethering of an acetylacetonate fragment on the surface of SiO_2-SH. Furthermore, TGA curves also provide an indirect evidence to support the covalently formation of the SiO_2-SH-DP that a sharp weight loss happened at a temperature higher than 350 ^oC, which can be explained by the decomposition of organic fragment on SiO_2-SH-DP. Interestingly, the total weight loss of SiO_2-SH-DP-Cu is decreased by 9% compared to SiO_2-SH-DP, we ascribed the reason to the shielding effect of the copper shell on the surface of SiO_2-SH-DP and the weight incremental influence which given by copper nanoparticle. XPS analysis with respect to the silica nanoparticle was also conducted. In the XPS pattern of the C 1s region, contributions of C-O (287.6 eV), C-C (285.1 eV), and C=C (284.2 eV) bonds can all be found in the sample of SiO_2-SH, which corresponds to the alkane chain in the chemical modified silica (**Fig. 4e**). After covalently reacted with DP, a new peak in 287.6 eV, which can be ascribed to the C=O, is observed in the XPS pattern (**Fig. 4g**). On the other hand, there is no observation of Cu peaks in the XPS spectra of SiO_2-SH, while, peaks at 732.5, 952.3 eV is found in SiO_2-SH-DP-Cu, proves the existence of Cu (**Fig. 4f and 4h**). Along with the Cu 2p response, the XPS data constituted a solid evidence that DP is linked on the skeleton of silica and Cu is also a key component in SiO_2-SH-DP-Cu.

With the chemical modified silica nanoparticle in hand, we initiated the study on its performance in nanofluids in terms of stability and some thermo-physical properties. In this work, we chose two representative DESs, glycerol (GL)/chlorine chloride (ChCl) and EG/ ChCl. As is well known, GL is a kind of green solvent which was mainly produced as a by-product of biodiesel. As the rapid expansion of biodiesel demand caused by shortage of fossil resource, a significant glut of global GL market is under continuous growing.[43] Thus, utilization GL, in particular for high value-added using has been becoming a bottleneck of the advance of biodiesel industry.[44, 45] Meanwhile, as a matter of fact, EG is a good alcohol type working fluid that has been widely adopted in both academia and industry owing to its low cost, accessibility and chemical stability.[46] Especially, the mixture of 40-50 *vol*% EG in water has been well recognized to be used as a coolant due to its low freezing point.[47,

[48] In addition, ChCl is also a bio-degradable chemical that was usually used as an animal food additive. Despite GL/ChCl and EG/ChCl DESs have been studied towards as base solvents of nanofluids, they usually restricted by poor stability and thermal conductivity.[32, 49] Therefore, nanoparticle that can be dispersed in DES with superior stability and thermal conductivity would be highly desirable. To verify the feasibility of the prepared silica nanoparticle, GL/ChCl DES based nanofluids were fabricated. Thermal conductivity of the nanofluids was firstly considered. To ease the influence of the testing uncertainties, thermal conductivity in a certain condition was tested for ten times, data described in following text was the average of the testing results. As shown in **Fig. 5a** and **5b**, thermal conductivity of GL/ChCl DES was observed to possess a maximum enhancement of 2.0% after dispersing 1.0 *wt*% of SiO_2-SH-DP-Cu nanoparticle, while SiO_2-SH and SiO_2-SH-DP dispersed nanofluids display only comparable thermal conductivity enhancement, clearly indicates the thermal conductive enhancement effect of copper decorated silica nanoparticle. Similar results can be observed in the case of EG/ChCl DES based nanofluids that silica containing copper exhibited an enhancement approximate 5.0%, while, the rest of other two silica nanoparticles show only 1.0-2.0% enhancement (**Fig. 5c** and **5d**). Further, thermal conductivity of GL/ChCl based nanofluids with different amount of SiO_2-SH-DP-Cu nanoparticle filler was studied. As it is seen in **Fig. 5e** and **5f**, thermal conductivity is increased significantly with the rising amount of nanofiller, 12.5% of thermal conductivity enhancement is observed when 5.0 *wt*% of nanoparticle was filled in the base solvent. On the other hand, SiO_2-SH-DP-Cu nanoparticle filled EG/ChCl also displays a remarkable 13.6% of thermal conductivity enhancement after blending 5.0 *wt*% of nanoparticle in the based DES. Comparing with the reported results summarized in table 2, nanofluids prepared by using this kind of hybrid silica composite displays an obvious superiority in terms of thermal conductivity. Moreover, to the best of our knowledge, this is the first example which adopts a silica into fabrication a DES based nanofluid. It is worth noting that these nanofluids exhibit promising stability that it can kept at ambient temperature for 15 days without observation of obvious precipitation thanks to the alkane chain on the surface of silica. Zeta potential value, the gravity settlement observation results as well as TEM images at different standing time were shown in the supporting information (SI) (**Fig. S1**).

Moreover, viscosity of the nanofluids was tested since pump power input in real application has

a great dependence on it, which thus deeply associates with the energy consumption. As it is displayed in **Fig. 6a**, the addition of 1.0 *wt*% chemical decorated SiO_2 nanofillers results in a slight viscosity decrease in GL/ChCl DES base solvent, the same phenomenon can be observed in EG/ChCl based solvent system. These uncommon experimental results demonstrated that the addition of nanoparticle could offer a positive effect on the decrease of viscosity. It is well recognized that viscosity of liquid is mainly determined by the interaction between the molecules.[50, 51] The decreasing of viscosity was mainly beneficial from interaction between nanoparticles and base solvent, which was mainly constituted by hydrogen bonding effect, thus the hydrogen bonding effect among base solvent molecule, a hydrogen donor component, would be partially ruined. Therefore we assumed that this interrupting effect that caused by the participation of nanoparticle was responsible for the decreasing of relative viscosity.

Viscosities of nanofluids with different mass fraction of nanofiller were then subjected to test. As shown in **Fig. 6c**, viscosities of nanofluids lies below GL/ChCl base solvent when 1.0 *wt*%, 2.0 *wt*% and 3.0 *wt*% of SiO_2-SH-DP-Cu were used as nanofiller, and the lowest viscosity value is found in the case of 3.0 *wt*% nanofluids. While the viscosities increase to some degree when the mass fraction of nanoparticle is more than 3.0 %. This result indicated that the shearing effect between nanofiller, which would lead to viscosity increase, has overwhelmed the intermolecular hydrogen bonding effect between nanofiller and base solvent. Therefore, viscosity of the whole nanofluids system was raised. The similar phenomenon was found in EG/ChCl DES based nanofluids, viscosity of nanofluids exhibited an decreasing trend in the initial stage, but rising up after dispersing a mass fraction of nanoparticle more than 2.0% (**Fig. 6d**). Notably, the hydrogen bonding interrupting effect in EG/ChCl DES system which caused by nanoparticle was weaker than that of GL/ChCl owing to its relatively low hydrogen bonding concentration. Therefore, viscosity enhancement phenomenon derived from nanoparticle becomes a dominating factor to impact the performance of the base solvent for EG/ChCl DES system. It should be noted that this uncommon phenomenon has actually been unveiled in literatures, in particular for those solvent system involving fertile intermolecular hydrogen bonding.[51]

After knowing the static characteristics of the as-prepared copper silica hybrid nanoparticle, the convective heat transfer coefficient *h* was submitted to study with the aim at understanding the flow

convective performance of the nanofluids. **Fig. 7a** is a schematic diagram of the experimental setup for testing the heat transfer performance of nanofluids, it is constituted by a nanofluids reservoir equipped with a magnetic stirrer, two pumps, a heat transfer test section, a water bath which severed as low temperature regulation unit, a flow meter, a tubular heat exchanger and a data acquisition system. Before the *h* testing experiment, some factors that related thermophysical properties were calculated. At the first, the density of nanofluids can be calculated as eqn (1) [52],

$$\rho_{nf} = (1-\varphi)\rho_{bf} + \varphi\rho_{Particle} \quad (1)$$

where ρ_{nf}, ρ_{bf} and ρ_p refer to the density of nanofluid, base fluid and nanoparticle, respectively. φ is volumetric fraction of nanoparticles. Assuming that the nanoparticle and the base solvent are in thermal equilibrium, the specific heat capacity of this type mixture can be obtained by eqn (2) [52],

$$c_{p,nf} = \frac{\rho_p}{\varphi\rho_{nf}} c_{p,Particle} + (1-\varphi)\frac{\rho_{bf}}{\rho_{nf}} c_{p,bf} \quad (2)$$

Where $c_{p,nf}$ represents the specific heat capacity of nanofluid, $c_{p,Particle}$ is the specific heat capacity of nanoparticle, and $c_{p,bf}$ is assigned to specific heat capacity of base fluid. Then the specific heat capacity of nanofluids can be calculated as eqn (3),

$$c_{p,nf} = \frac{\varphi\rho_p c_{p,Particle} + (1-\varphi)\rho_{bf} c_{p,bf}}{(1-\varphi)\rho_{bf} + \varphi\rho_p} \quad (3)$$

The average heat transfer rate of working fluids in the Q_{nf} can be calculated as:

$$Q_{nf} = q_v \rho_{nf} c_{p,nf} (t_{out} - t_{in}) \quad (4)$$

where q_v is the volumetric flow rate of nanofluids, t_{out} and t_{in} are the output and input temperature of nanofluids respectively, and it can be converted to mass flow rate after multiplying the density of nanofluids, thus Q_{nf} can be calculated as eqn (5):

$$Q_{nf} = q_{nf} c_{p,nf} (t_{out} - t_{in}) \quad (5)$$

Eqn (9) is used to verify the inner temperature of flow pipeline, where λ refers to thermal conductivity of copper, $t_{w,o}$ and $t_{w,i}$ are the outside and inner temperature of tube respectively, *U* and *I* represent the electricity voltage and current displayed in the controller.

$$\emptyset = \frac{2\pi\lambda(t_{w,o} - t_{w,i})}{ln\frac{d_o}{d_i}} = UI \quad (6)$$

$t_{w,i}$ can be obtained according to eqn (6), thus, the average convective heat transfer coefficient *h* can be calculated using the Newton cooling eqn (7), where t_f is the average temperature of nanofluids

in the testing tube and it is the mean value of output and input temperature of nanofluids (eqn (8)).

$$h = \frac{Q_{nf}}{\pi d_i (t_{w,i} - t_f)} \quad (7)$$

$$t_f = \frac{t_{out} + t_{in}}{2} \quad (8)$$

$$Re = \frac{u d_i}{\nu} = \frac{\rho_{nf} d_i}{\mu} \cdot u = \frac{\rho_{nf} d_i}{\mu} \cdot \frac{q_v}{\frac{\pi}{4} d_i^2} \quad (9)$$

According to the above equations, thermo-physical properties of different types silica filled EG/ChCl DES based nanofluids were shown in table 3. To facilitate the comparison among different nanofluids and base solvents, we fixed the base solvent of nanofluids at EG/ChCl = 3:1, the mass fraction of nanoparticle at 1.0%. As it is presented in **Fig. 7b** the convective heat transfer coefficients of nanofluids are much higher than that of base solvent regardless of Reynolds number. In the low Reynold number range, SiO_2-SH displays the optimum convective heat transfer performance mainly due to the relatively smaller size of the SiO_2-SH compared with the other two chemical modified, for which, a more dynamic Brownian motion could be theoretically expected. While, as the increase of Reynold number, SiO_2-SH-DP-Cu filled nanofluids affords the superior convective heat transfer coefficient over the rest of two kinds of nanofluids that a 24.9% heat transfer coefficient enhancement was obtained compared with that of base solvent at a Reynolds number of 1400. This phenomenon further proves that the chemical modified silica nanoparticles filled nanofluids not only displays a better thermo-physical performance regarding static state, but also the convective heat transfer in a dynamic condition is beneficial from the existence of Cu on the surface of silica owing to the thermal conductivity enhancement effect.

In order to understand the deep mechanism responsible for the stability improvement of SiO_2-SH-DP in glycerol, a molecular dynamic simulation was conducted by using SiO_2 nanoparticle as a comparison sample. The molecular dynamic simulations method was demonstrated in supporting information (SI). As it is shown in **Fig. 8a** and **8b**, interface interactions between SiO_2, SiO_2-SH-DP and glycerol molecule were taken into account, the bottom part stands for the surface of nanoparticle and the upper dispersing molecule represents the solvent of GL. The number of vicinal oxygen atom on the surface of nanoparticles as a function of radial distribution was plotted in **Fig. 8c**, the area blow the curve thus means the coordinate effect of GL on the vicinal of SiO_2 nanoparticles, it is obvious that the coordination effect between liquid and solid interface becomes

stronger after covalent modification of alkane chain, which clearly proves that affinity between nanoparticle and solvent is improved owing to the existence of alkane chain. In addition, the diffusion coefficient significantly decreases after decorating with the alkane chain (table 4), which also supports the assumption that interaction between SiO_2-SH-DP and glycerol was enhanced compared with that of SiO_2 and glycerol molecule. Hydrogen bond lifetime analysis regarding glycerol molecule provides another evidence to the interaction between solid and liquid phase since it increases from 539.563 fs to 541.798 fs after alkane modification which means that the alkane chain renders the increment of hydrogen bond interaction thanks to the contribution of interaction between nanoparticle and solvent molecule. Hence, all of the data obtained from molecular dynamic simulation could support our hypothesis that the affinity of SiO_2 and glycerol was much improved due to grafting of alkane chain on its surface, which in turn resulted in the enhancement of stability of the as-prepared nanofluids.

Conclusions

A chemically decorated silica filled DES based nanofluid that could fulfill both thermal conductivity enhancement and static stability was fabricated by rendering DP derivative as a covalently linker with the aid of catalytic amount of Lewis acid. DP was employed as dual alkane brush and metal nanoparticle anchor to ensure the superior performance of SiO_2-SH-DP-Cu in DES base solvent system. This work represent the concept of sustainability well since the main raw material, DP, is made from a convenient three-component reaction in water, and DESs are also produced from environmental benign solvents and chemicals. Moreover, the synthesized nanofluids were applied into energy transfer. 12.5% and 13.6% thermal conductivity were achieved in GL/ChCl and EG/ChCl DES system respectively with a promising stability. The mechanism responsible for stability enhancement was evidenced by a molecular dynamic simulation that the intermolecular hydrogen bonding effect between base solvent and nanoparticle has an important role. Given the wide liquid range, high static thermal conductivity and convective heat transfer efficiency, nanofluids developed in this article bearing a great potential for further thermal management and energy harvesting application field.

Experimental section

Materials

Unless otherwise noted, the reagents were used as received without further purification. Pure anhydrous glycerol (99.8%) and (3-mercaptopropyl)trimethoxysilane (99.0%) were purchased from Shanghai Aladdin Bio-Chem Technology Co., Ltd. Choline chloride, EG (99.8%), tetraethyl orthosilicate (TEOS) were purchased from National Medicines Corporation Ltd. China. SiC and Fe_3O_4 were purchased from Nanjing Xianfeng Nanotechnology Company. *n*-Hexadecylamine was purchased from Tokyo Chemical industry Co., Ltd (TCI), Japan. Cupric acetylacetonate was purchased from Sigma-Aldrich Company.

FT-IR spectra were recorded using a Bruker VERTEX 70 FT-IR as KBr discs. Thermal gravimetric analysis (TGA) was carried out on a TA SDT Q600 instrument under a nitrogen atmosphere by heating from room temperature to 800 °C at a rate of 10 °C min^{-1}. X-ray diffraction (XRD) patterns were recorded on a diffractometer (Smartlab, Rigaku) with Ni-filtered CuK α radiation (k = 0.154 nm) at a tube current of 30 mA and a generator voltage of 40 kV. Scanning was performed at a speed of 8 °C min^{-1}, from 0 to 80° of 2θ. The viscosities of nanofluids were measured by digital rotary viscometer (NDJ-79B, Shanghai changji geological instrument Co.LTD, China). The thermal conductivities were measured by a Xiatech TC3000L liquid thermal conductivity analyzer, the testing temperature was adjusted and controlled by a water bath and an insulated chamber. X-ray photoelectron spectra (XPS) were recorded on a SHIMADZU-Kratos AXIS-ULTRA DLD-600W X-ray photoelectron spectrometer at a base pressure of 2×10^{-9} Pa in the analysis chamber using Al Kα radiation. Scanning electron microscopy (SEM) images were recorded using a FEI Sirion 200 field-emission scanning electron microscope operating at 10 kV. Transmission electron microscopy (TEM) were recorded using a FEI Tecnai G2 F20 equipped with an X-ray energy dispersive spectroscopy (EDS).

Uncertainty analysis

Uncertainty analysis is taken into account. Due to the uncertainty of the data acquisition device and thermocouples, the temperature measurement error range for each measuring point is ±0.5 °C. The accuracy of rotary viscometer is ±3% at a working temperature from 0 to 100 °C. The thermal

conductivity analyser has an accuracy of ±3% at a working temperature from -200 to 150 °C.

Preparation of SiO_2-SH

To a 250 ml round bottom flask, *n*-hexadecylamine (3.31 mmol, 0.8 g) was dissolved at room temperature in an aqueous mixture of water (18 mL) and ethanol (21 mL). Then, tetraethoxysilane (TEOS, 0.039mol, 4.15 g) and (3-mercaptopropyl)trimethoxysilane (MPTMS, 1.97 g, 0.01 mol) were premixed in ethanol (14 mL) and simultaneously dropped in the reaction mixture through a dropping funnel at a 50 °C reaction temperature. The mixture was allowed to stir for another 20 h. After completion of the reaction, the resulting mixture was subjected to filtration to obtain a white powder raw silica material. The final SiO_2-SH nanomaterial (1.89 g) was gained after a soxhlet washing with methanol as solvent for 48 h and drying in a 60 °C oven for 18 h.

Preparation of SiO_2-SH-DP

To a 100 mL round bottom flask, SiO_2-SH (2.0) was mixed with DP (4.0 mmol, 0.85 g) and $ZnCl_2$ (0.8 mmol, 0.109 g) in acetonitrile (20 mL). The mixture was heated to 80 °C and stirred at that temperature for 10 h. After the completion of reaction, the mixture was then undergone a filtration and ethanol washing for three times. SiO_2-SH-DP (2.42 mg) was obtained as a white powder after drying for 18 h in a 60 °C oven.

Preparation of SiO_2-SH-DP-Cu

To a 100mL round bottom flask, SiO_2-SH-DP (0.5 g) was mixed with $Cu(acac)_2$ (0.2 mmol, 52.0 mg) in ethanol (20 mL). The mixture was heated to 70 °C and stirred at that temperature for 24 h. $NaBH_4$ (6.873 mmol, 260 mg) was added into the reaction in one portion, the solution was continued to stir at the same temperature for another 24 h. SiO_2-SH-DP-Cu (349.8 mg) was obtained as a white powder after drying for 18 h in a 60 °C oven.

Preparation of GL/ChCl DES[32]

The reaction was conducted in a 500 mL round bottom flask with a magnetic stirrer. GL (150 g, 1.63 mol) was mixed with ChCl (75.5 g, 0.54 mol).The mixture was heated to 100 °C and allowed to stir for 1 h. GL/ChCl DES was obtained after cooling the mixture to room temperature. Unless otherwise noted the mole ratio of GL to ChCl and GC to ChCl was 3:1 in this paper.

A typical preparation procedure of nanofluids

The reaction was conducted in a 50 mL glass sealed tube with a magnetic stirrer. GL/ChCl DES

(100 mL) was mixed with silica nanoparticle (varied according to the mass fraction of the nanofiller), the mixture was then heated to 80 °C and allowed to stir for 2 h. After reaction, the mixture was cooled to room temperature. Subsequently, the solution was subjected to sonication (53 KHz) for 2 h to obtain the final nanofluid.

Supporting Information

The Supporting Information is available free of charge on the ACS Publications website. Molecular dynamic Simulations method in **S2.** Stability study of chemically decorated silica filled DES based nanofluids in **Figure S1.** XPS survey spectra of (a) SiO_2-SH, (b) SiO_2-SH-DP and (c) SiO_2-SH-DP-Cu respectively in **Figure S2.** NMR data and spectra of 1-(2-butoxy-6-methyl-3,4-dihydro-2H-pyran-5-yl)ethanone in **Figure S3.**

Conflicts of interest

There are no conflicts to declare.

Acknowledgements

Thanks for financial support from the National Natural Science Foundation of China (No. 51776218, 51906252), the Fundamental Research Funds for the Central Universities (No. 2019XKQYMS69) is also acknowledged.

Reference

1. Sun, J.; Fu, L.; Zhang, S., A review of working fluids of absorption cycles. *Renewable Sustainable Energy Rev.* **2012,** *16* (4), 1899-1906.

2. Chen, H.; Goswami, D. Y.; Stefanakos, E. K., A review of thermodynamic cycles and working fluids for the conversion of low-grade heat. *Renewable Sustainable Energy Rev.* **2010,** *14* (9), 3059-3067.

3. Navas, J.; Martinez-Merino, P.; Sanchez-Coronilla, A.; Jesus Gallardo, J.; Alcantara, R.; Martin, E. I.; Pinero, J. C.; Leon, J. R.; Aguilar, T.; Hidalgo Toledo, J.; Fernandez-Lorenzo, C., MoS2 nanosheets vs. nanowires: preparation and a theoretical study of highly stable and efficient nanofluids for concentrating solar power. *J. Mater. Chem. A* **2018,** *6* (30), 14919-14929.

4. Xu, X.; Peng, C.; Cao, G.; Liu, H.; Hu, Y., Application of a New Lattice-Fluid Equation of State Based on Chemical-Association Theory for Polymer Systems. *Ind. Eng. Chem. Res.* **2009,** *48* (16), 7828-7837.

5. Zaera, F., Nanostructured materials for applications in heterogeneous catalysis. *Chem. Soc. Rev.* **2013,** *42* (7), 2746-2762.

6. Zhang, X.; Pan, L.; Wang, L.; Zou, J.-J., Review on synthesis and properties of high-energy-density liquid fuels: Hydrocarbons, nanofluids and energetic ionic liquids. *Chem. Eng. Sci.* **2018,** *180*, 95-125.

7. Gomez-Villarejo, R.; Navas, J.; Martin, E. I.; Sanchez-Coronilla, A.; Aguilar, T.; Jesus Gallardo, J.; De los Santos, D.; Alcantara, R.; Fernandez-Lorenzo, C.; Martin-Calleja, J., Preparation of Au nanoparticles in a non-polar medium: obtaining high-efficiency nanofluids for

concentrating solar power. An experimental and theoretical perspective. *J. Mater. Chem. A* **2017,** *5* (24), 12483-12497.

8. Choi, S. U. S., Nanofluids: From Vision to Reality Through Research. *J. Heat Transfer* **2009***,131*(3), No. 033106.

9. Jang, S. P.; Choi, S. U. S., Role of Brownian motion in the enhanced thermal conductivity of nanofluids. *Appl.Phys. Lett.* **2004,** *84* (21), 4316-4318.

10. Eastman, J. A.; Choi, S. U. S.; Li, S.; Yu, W.; Thompson, L. J., Anomalously increased effective thermal conductivities of ethylene glycol-based nanofluids containing copper nanoparticles. *Appl.Phys. Lett.* **2001,** *78* (6), 718-720.

11. Do, K. H.; Jang, S. P., Effect of nanofluids on the thermal performance of a flat micro heat pipe with a rectangular grooved wick. *Int. J. Heat Mass Transfer* **2010,** *53* (9-10), 2183-2192.

12. Brites, C. D. S.; Xie, X.; Debasu, M. L.; Qin, X.; Chen, R.; Huang, W.; Rocha, J.; Liu, X.; Carlos, L. D., Instantaneous ballistic velocity of suspended Brownian nanocrystals measured by upconversion nanothermometry. *Nature Nanotech.* **2016,** *11* (10), 851-856.

13. Wang, B.; Wang, X.; Lou, W.; Hao, J., Rheological and Tribological Properties of Ionic Liquid-Based Nanofluids Containing Functionalized Multi-Walled Carbon Nanotubes. *J. Phys. Chem. C* **2010,** *114* (19), 8749-8754.

14. Liu, J.; Ye, Z.; Zhang, L.; Fang, X.; Zhang, Z., A combined numerical and experimental study on graphene/ionic liquid nanofluid based direct absorption solar collector. *Sol. Energy Mater. Sol. Cells.* **2015,** *136*, 177-186.

15. Kong, C.; Qian, W.; Zheng, C.; Fei, W., Enhancing 5 V capacitor performance by adding single walled carbon nanotubes into an ionic liquid electrolyte. *J. Mater. Chem. A* **2015,** *3* (31), 15858-15862.

16. Tian, H.; Du, L.; Huang, C.; Wei, X.; Lu, J.; Wang, W.; Ding, J., Enhanced specific heat capacity of binary chloride salt by dissolving magnesium for high-temperature thermal energy storage and transfer. *J. Mater. Chem. A* **2017,** *5* (28), 14811-14818.

17. Zhang, Q.; De Oliveira Vigier, K.; Royer, S.; Jerome, F., Deep eutectic solvents: syntheses, properties and applications. *Chem. Soc. Rev.* **2012,** *41* (21), 7108-46.

18. Wagle, D. V.; Zhao, H.; Baker, G. A., Deep eutectic solvents: sustainable media for nanoscale and functional materials. *Acc. Chem. Res.* **2014,** *47* (8), 2299-308.

19. Mou, H.; Wang, J.; Yu, D.; Zhang, D.; Lu, F.; Chen, L.; Wang, D.; Mu, T., A facile and controllable, deep eutectic solvent aided strategy for the synthesis of graphene encapsulated metal phosphides for enhanced electrocatalytic overall water splitting. *J. Mater. Chem. A* **2019,** *7* (22), 13455-13459.

20. Ghorpade, U. V.; Suryawanshi, M. P.; Shin, S. W.; Kim, J.; Kang, S. H.; Ha, J.-S.; Kolekar, S. S.; Kim, J. H., Unassisted visible solar water splitting with efficient photoelectrodes sensitized by quantum dots synthesized via an environmentally friendly eutectic solvent-mediated approach. *J. Mater. Chem. A* **2018,** *6* (45), 22566-22579.

21. Smith, E. L.; Abbott, A. P.; Ryder, K. S., Deep eutectic solvents (DESs) and their applications. *Chem. Rev.* **2014,** *114* (21), 11060-82.

22. Fang, Y. K.; Osama, M.; Rashmi, W.; Shahbaz, K.; Khalid, M.; Mjalli, F. S.; Farid, M.

M., Synthesis and thermo-physical properties of deep eutectic solvent-based graphene nanofluids. *Nanotechnology* **2016,** *27* (7), 075702.

23. Chen, Y. Y.; Walvekar, R.; Khalid, M.; Shahbaz, K.; Gupta, T. C. S. M., Stability and thermophysical studies on deep eutectic solvent based carbon nanotube nanofluid. *Mater. Res. Express* **2017,** *4* (7), 075028.

24. Martins, M. A. R.; Crespo, E. A.; Pontes, P. V. A.; Silva, L. P.; Bülow, M.; Maximo, G. J.; Batista, E. A. C.; Held, C.; Pinho, S. P.; Coutinho, J. A. P., Tunable Hydrophobic Eutectic Solvents Based on Terpenes and Monocarboxylic Acids. *ACS Sustainable Chem. Eng.* **2018,** *6* (7), 8836-8846.

25. Dietz, C. H. J. T.; Creemers, J. T.; Meuleman, M. A.; Held, C.; Sadowski, G.; van Sint Annaland, M.; Gallucci, F.; Kroon, M. C., Determination of the Total Vapor Pressure of Hydrophobic Deep Eutectic Solvents: Experiments and Perturbed-Chain Statistical Associating Fluid Theory Modeling. *ACS Sustainable Chem. Eng.* **2019,** *7* (4), 4047-4057.

26. Altamash, T.; Amhamed, A. I.; Aparicio, S.; Atilhan, M., Combined Experimental and Theoretical Study on High Pressure Methane Solubility in Natural Deep Eutectic Solvents. *Ind. Eng. Chem. Res.* **2019,** *58* (19), 8097-8111.

27. Sirvio, J. A., Fabrication of regenerated cellulose nanoparticles by mechanical disintegration of cellulose after dissolution and regeneration from a deep eutectic solvent. *J. Mater. Chem. A* **2019,** *7* (2), 755-763.

28. Abo-Hamad, A.; Hayyan, M.; AlSaadi, M. A.; Hashim, M. A., Potential applications of deep eutectic solvents in nanotechnology. *Chem. Eng. J.* **2015,** *273*, 551-567.

29. Abdullah, M.; Malik, S. R.; Iqbal, M. H.; Sajid, M. M.; Shad, N. A.; Hussain, S. Z.; Razzaq, W.; Javed, Y., Sedimentation and stabilization of nano-fluids with dispersant. *Colloid Surf. Physicochem. Eng. Asp.* **2018,** *554*, 86-92.

30. Yu, W.; Xie, H.; Wang, X.; Wang, X., Significant thermal conductivity enhancement for nanofluids containing graphene nanosheets. *Phys. Lett. A* **2011,** *375* (10), 1323-1328.

31. Yu, W.; Xie, H., A Review on Nanofluids: Preparation, Stability Mechanisms, and Applications. *J. Nanomater.* **2012,** *2012*, 1-17.

32. Liu, C.; Fang, H.; Qiao, Y.; Zhao, J.; Rao, Z., Properties and heat transfer mechanistic study of glycerol/choline chloride deep eutectic solvents based nanofluids. *Int. J. Heat Mass Transfer* **2019,** *138*, 690-698.

33. Branson, B. T.; Beauchamp, P. S.; Beam, J. C.; Lukehart, C. M.; Davidson, J. L., Nanodiamond Nanofluids for Enhanced Thermal Conductivity. *ACS Nano* **2013,** *7* (4), 3183-3189.

34. Liu, J.; Xu, C.; Chen, L.; Fang, X.; Zhang, Z., Preparation and photo-thermal conversion performance of modified graphene/ionic liquid nanofluids with excellent dispersion stability. *Sol. Energy Mater. Sol. Cells.* **2017,** *170*, 219-232.

35. Liu, C.; Huang, W.; Wang, M.; Pan, B.; Gu, Y., Expedient Synthesis of Substituted Benzoheterocycles using 2-Butoxy-2,3-dihydrofurans as 4+2 Benzannulation Reagents. *Adv. Synth. Catal.* **2016,** *358* (14), 2260-2266.

36. Liu, C.; Zhou, L.; Jiang, D.; Gu, Y., Multicomponent Reactions of Aldo-X Bifunctional

Reagent -Oxoketene Dithioacetals and Indoles or Amines: Divergent Synthesis of Dihydrocoumarins, Quinolines, Furans, and Pyrroles. *Asian J. Org. Chem.* **2016,** *5* (3), 367-372.

37. Liu, C.; Zhou, L.; Huang, W.; Wang, M.; Gu, Y., Synthesis of Furans and Pyrroles from 2-Alkoxy-2,3-dihydrofurans Through a Nucleophilic Substitution-Triggered Heteroaromatization. *Adv. Synth. Catal.* **2016,** *358* (6), 900-918.

38. Liu, C.; Pan, B.; Gu, Y., Lewis base-assisted Lewis acid-catalyzed selective alkene formation via alcohol dehydration and synthesis of 2-cinnamyl-1,3-dicarbonyl compounds from 2-aryl-3,4-dihydropyrans. *Chinese J. Catal.* **2016,** *37* (6), 979-986.

39. Liu, C.; Taheri, A.; Lai, B.; Gu, Y., Synergistic catalysis-induced ring-opening reactions of 2-substituted 3,4-dihydropyrans with alpha-oxoketene dithioacetals. *Catal. Sci. Technol.* **2015,** *5* (1), 234-245.

40. Li, M.; Li, H.; Li, T.; Gu, Y., Ring-Opening Reactions of 2-Alkoxy-3, 4-dihydropyrans with Thiols or Thiophenols. *Org. Lett.* **2011,** *13* (5), 1064-1067.

41. Gu, Y.; De Sousa, R.; Frapper, G.; Bachmann, C.; Barrault, J.; Jérôme, F., Catalyst-free aqueous multicomponent domino reactions from formaldehyde and 1,3-dicarbonyl derivatives. *Green Chem.* **2009,** *11* (12), 1968–1972.

42. Lai, B.; Huang, Z.; Jia, Z.; Bai, R.; Gu, Y., Silica-supported metal acetylacetonate catalysts with a robust and flexible linker constructed by using 2-butoxy-3,4-dihydropyrans as dual anchoring reagents and ligand donors. *Catal. Sci. Technol.* **2016,** *6* (6), 1810-1820.

43. Monteiro, M. R.; Kugelmeier, C. L.; Pinheiro, R. S.; Batalha, M. O.; Cesar, A. d. S., Glycerol from biodiesel production: Technological paths for sustainability. *Renewable Sustainable Energy Rev.* **2018,** *88*, 109-122.

44. Okoye, P. U.; Abdullah, A. Z.; Hameed, B. H., A review on recent developments and progress in the kinetics and deactivation of catalytic acetylation of glycerol-A byproduct of biodiesel. *Renewable Sustainable Energy Rev.* **2017,** *74*, 387-401.

45. He, Q.; McNutt, J.; Yang, J., Utilization of the residual glycerol from biodiesel production for renewable energy generation. *Renewable Sustainable Energy Rev.* **2017,** *71*, 63-76.

46. Sohel Murshed, S. M.; Nieto de Castro, C. A., Conduction and convection heat transfer characteristics of ethylene glycol based nanofluids - A review. *Appl. Energ.* **2016,** *184*, 681-695.

47. Hussein, A. M.; Kadirgama, K.; Noor, M. M., Nanoparticles suspended in ethylene glycol thermal properties and applications: An overview. *Renewable Sustainable Energy Rev.* **2017,** *69*, 1324-1330.

48. Azmi, W. H.; Hamid, K. A.; Usri, N. A.; Mamat, R.; Sharma, K. V., Heat transfer augmentation of ethylene glycol: water nanofluids and applications - A review. *Int. Commun. Heat Mass Transfer* **2016,** *75*, 13-23.

49. Li, F.; Li, L.; Zhong, G.; Zhai, Y.; Li, Z., Effects of ultrasonic time, size of aggregates and temperature on the stability and viscosity of Cu-ethylene glycol (EG) nanofluids. *Int. J. Heat Mass Transfer* **2019,** *129*, 278-286.

50. Christensen, G.; Younes, H.; Hong, H.; Smith, P., Effects of solvent hydrogen bonding, viscosity, and polarity on the dispersion and alignment of nanofluids containing Fe2O3 nanoparticles. *J. Appl. Phys.* **2015,** *118* (21), 214302.

51. Yin, Y.; Ma, L.; Wen, S.; Luo, J., Fracture of the Intermolecular Hydrogen Bond Network Structure of Glycerol Modified by Carbon Nanotubes. *J.Phys. Chem. C* **2018,** *122* (34), 19931-19936.

52. Fan, X.; Chen, H.; Ding, Y.; Plucinski, P. K.; Lapkin, A. A., Potential of 'nanofluids' to further intensify microreactors. *Green Chem.* **2008,** *10* (6), 670-677.

53. Hwang, Y. J.; Ahn, Y. C.; Shin, H. S.; Lee, C. G.; Kim, G. T.; Park, H. S.; Lee, J. K., Investigation on characteristics of thermal conductivity enhancement of nanofluids. *Curr. Appl. Phys.* **2006,** *6* (6), 1068-1071.

54. Iqbal, S. M.; Raj, C. S.; Michael, J. J.; Irfan, A. M., A COMPARATIVE INVESTIGATION OF Al2O3/H2O, SiO2/H2O AND ZrO2/H2O NANOFLUID FOR HEAT TRANSFER APPLICATIONS. *Dig. J.Nanomater. Biostruct.* **2017,** *12* (2), 255-263.

55. Yan, S. Y.; Zhang, H. Y.; Wang, F.; Ma, R.; Wu, Y. T.; Tian, R., Analysis of thermophysical characteristic of SiO2/water nanofluid and heat transfer enhancement with field synergy principle. *J. Renewable Sustainable Energy* **2018,** *10* (6), 063704.

56. Xie, H.; Wang, J.; Xi, T.; Liu, Y., Thermal conductivity of suspensions containing nanosized SiC particles. *Int. J. Thermophys.* **2002,** *23* (2), 571-580.

57. Pryazhnikov, M. I.; Minakov, A. V.; Rudyak, V. Y.; Guzei, D. V., Thermal conductivity measurements of nanofluids. *Int. J. Heat Mass Transfer* **2017,** *104*, 1275-1282.

58. Ferrouillat, S.; Bontemps, A.; Ribeiro, J. P.; Gruss, J. A.; Soriano, O., Hydraulic and heat transfer study of SiO2/water nanofluids in horizontal tubes with imposed wall temperature boundary conditions. *Int. J. Heat Fluid Flow* **2011,** *32* (2), 424-439.

59. Darvanjooghi, M. H. K.; Esfahany, M. N., Experimental investigation of the effect of nanoparticle size on thermal conductivity of in-situ prepared silica-ethanol nanofluid. *Int. Commun. Heat Mass Transfer* **2016,** *77*, 148-154.

60. Akilu, S.; Baheta, A. T.; Minea, A. A.; Sharma, K. V., Rheology and thermal conductivity of non-porous silica (SiO2) in viscous glycerol and ethylene glycol based nanofluids. *Int. Commun. Heat Mass Transfer* **2017,** *88*, 245-253.

61. Guo, W. W.; Li, G. N.; Zheng, Y. Q.; Dong, C., Measurement of the thermal conductivity of SiO2 nanofluids with an optimized transient hot wire method. *Thermochim. Acta* **2018,** *661*, 84-97.

Figure captions:

Fig. 1 A logical research thread of this work.

Fig. 2 (a) Schematic illustration of the DP and Cu nanoparticle modified SiO_2 nanoparticle, (b) preparation procedure and conditions of SiO_2-SH, SiO_2-SH-DP and SiO_2-SH-DP-Cu.

Fig. 3 SEM image of (a) SiO_2-SH, (b) SiO_2-SH-DP, (c) SiO_2-SH-DP-Cu; TEM image of (d) SiO_2-SH, (e) SiO_2-SH-DP, (f) SiO_2-SH-DP-Cu; TEM image of (g) SiO_2-SH, (h) SiO_2-SH-DP, (i) SiO_2-SH-DP-Cu; (j) EDS elemental mapping of SiO_2-SH-DP-Cu.

Fig. 4 (a) XRD, (b) FT-IR, (c) ^{13}C MAS NMR, (d) TGA spectra of the as-prepared chemical modified silica; XPS spectra of SiO_2-SH-DP in the region of (e) C 1s and (f) Cu 2p; XPS spectra of SiO_2-SH-DP-Cu in the region of (g) C 1s and (h) Cu 2p.

Fig. 5 Thermal conductivity (a) and thermal conductivity enhancement (b) of GL/ChCl based nanofluids with different types of nanofillers; thermal conductivity (c) and thermal conductivity enhancement (d) of EG/ChCl based nanofluids with different types of nanofillers; thermal conductivity (e) and thermal conductivity enhancement (f) of GL/ChCl based nanofluids with different mass fraction of SiO_2-SH-DP-Cu; thermal conductivity (g) and thermal conductivity enhancement (h) of EG/ChCl based nanofluids with different mass fraction of SiO_2-SH-DP-Cu.

Fig. 6 Viscosity of (a) GL/ChCl and (b) EG/ChCl based nanofluids with different types of nanofillers; viscosity of (c) GL/ChCl and (d) EG/ChCl based nanofluids with different mass fraction of SiO_2-SH-DP-Cu.

Fig. 7 (a) Schematic diagram of convective heat transfer coefficient testing platform, (b) convective heat transfer coefficient as a function of Reynolds number.

Fig. 8 Molecule model description of (a) SiO_2/glycerol system, (b) SiO_2-SH-DP/glycerol system, (c) the number of vicinal oxygen atom on the surface of nanoparticles as a function of radial distribution.

Table captions:

Table 1 Summary of silica nanoparticles in this work.

Table 2 Some reported results on the thermal conductivity performance of silica filled nanofluids.

Table 3 Some related thermo-physical parameters of EG/ChCl based nanofluids.

Table 4 The diffusion coefficient and lifetime of SiO_2/glycerol heterogeneous system.

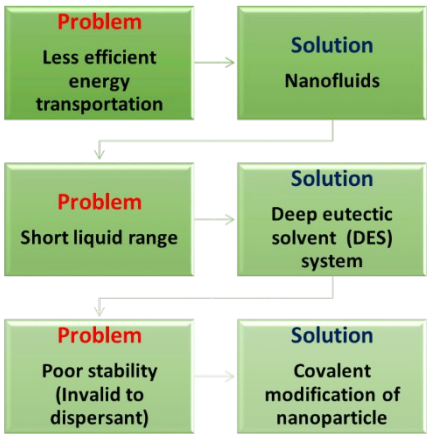

Fig. 1 A logical research thread of this work.

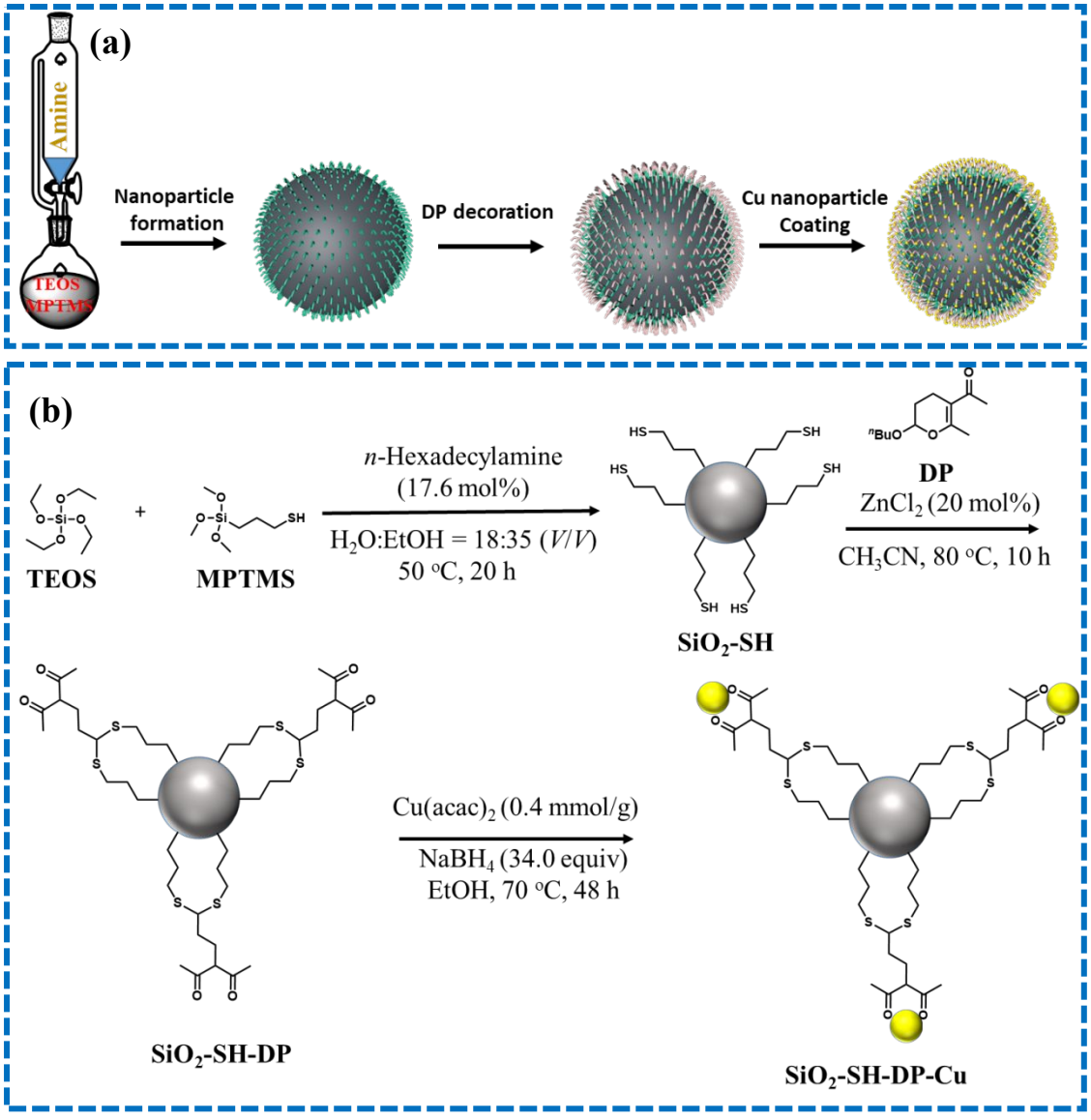

Fig. 2 (a) Schematic illustration of the DP and Cu nanoparticle modified SiO_2 nanoparticle, (b) preparation procedure and conditions of SiO_2-SH, SiO_2-SH-DP and SiO_2-SH-DP-Cu.

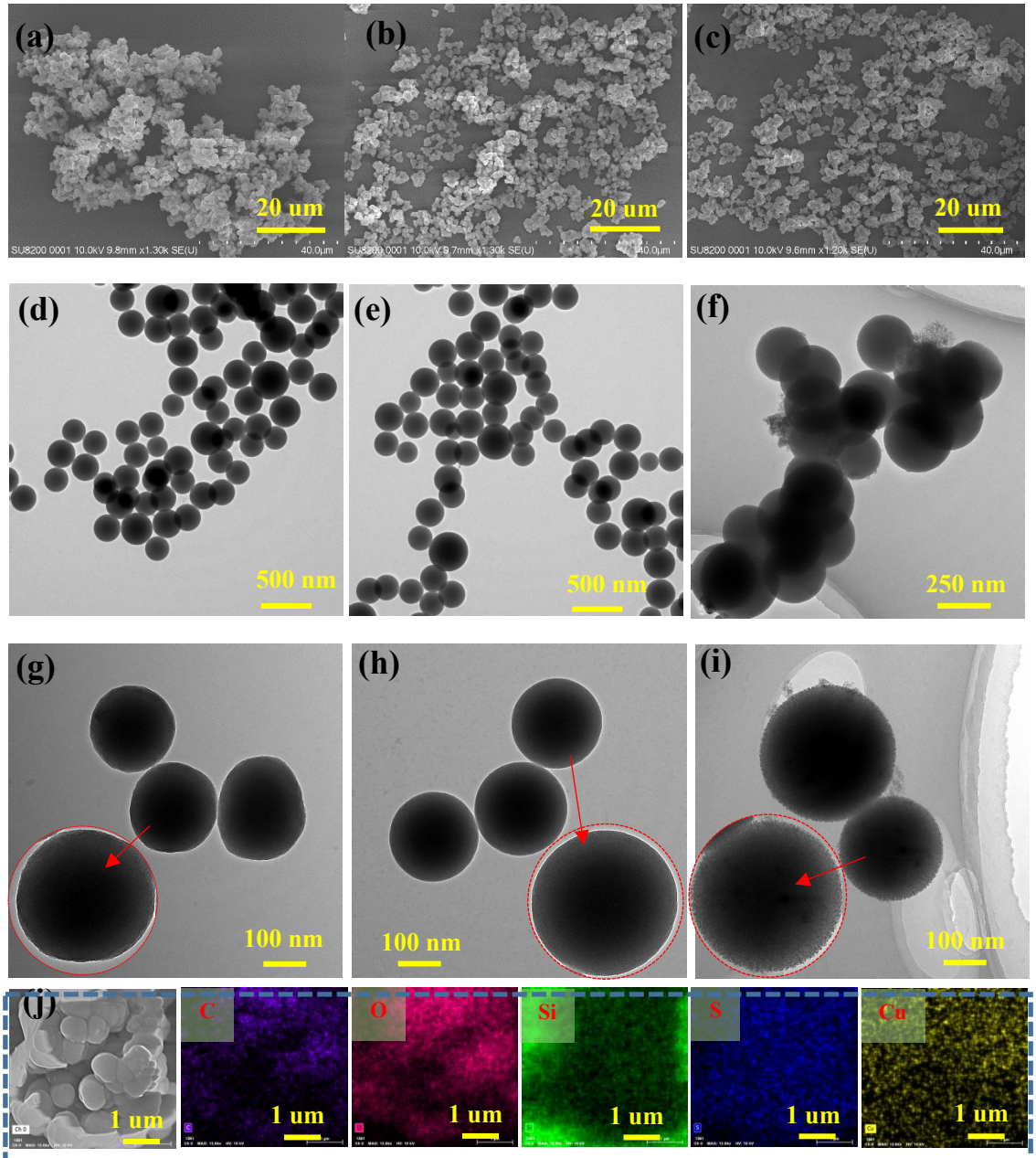

Fig. 3 SEM image of (a) SiO_2-SH, (b) SiO_2-SH-DP, (c) SiO_2-SH-DP-Cu, TEM image of (d) SiO_2-SH, (e) SiO_2-SH-DP, (f) SiO_2-SH-DP-Cu; TEM image of (g) SiO_2-SH, (h) SiO_2-SH-DP, (i) SiO_2-SH-DP-Cu; (j) EDS elemental mapping of SiO_2-SH-DP-Cu.

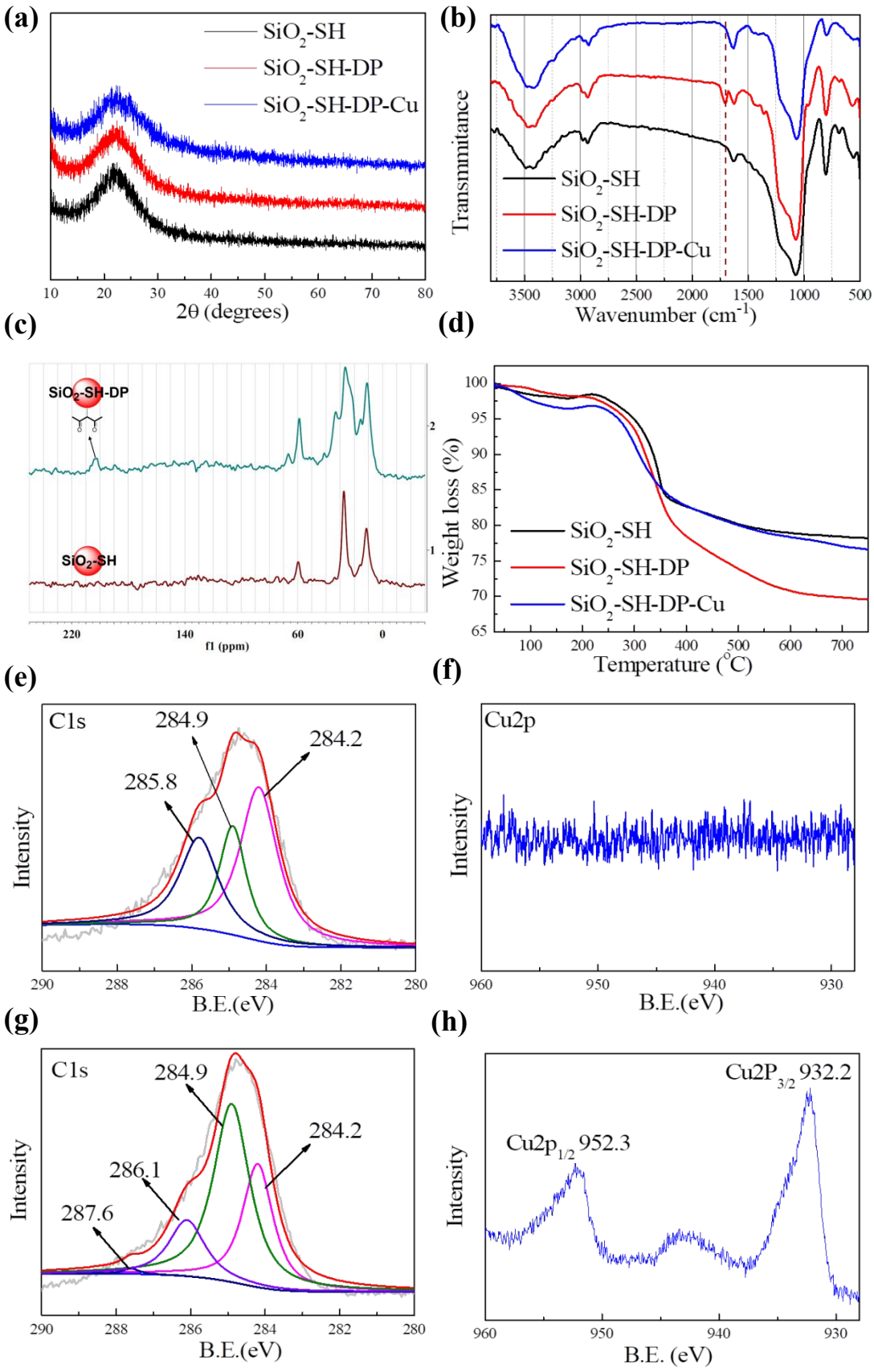
(a)
SiO2-SH
SiO2-SH-DP
SiO2-SH-DP-Cu
2θ (degrees)
(b)
Transmmitance
SiO2-SH
SiO2-SH-DP
SiO2-SH-DP-Cu
Wavenumber (cm-1)
(c)
SiO2-SH-DP
SiO2-SH
f1 (ppm)
(d)
Weight loss (%)
SiO2-SH
SiO2-SH-DP
SiO2-SH-DP-Cu
Temperature (°C)
(e)
C1s
284.9
284.2
285.8
Intensity
B.E.(eV)
(f)
Cu2p
Intensity
B.E.(eV)
(g)
C1s
284.9
284.2
286.1
287.6
Intensity
B.E.(eV)
(h)
Cu2P3/2 932.2
Cu2p1/2 952.3
Intensity
B.E. (eV)

Fig. 4 (a) XRD, (b) FT-IR, (c) ^{13}C MAS NMR, (d) TGA spectra of the as-prepared chemical modified silica; XPS spectra of SiO_2-SH-DP in the region of (e) C 1s and (f) Cu 2p; XPS spectra of SiO_2-SH-DP-Cu in the region of (g) C 1s and (h) Cu 2p.

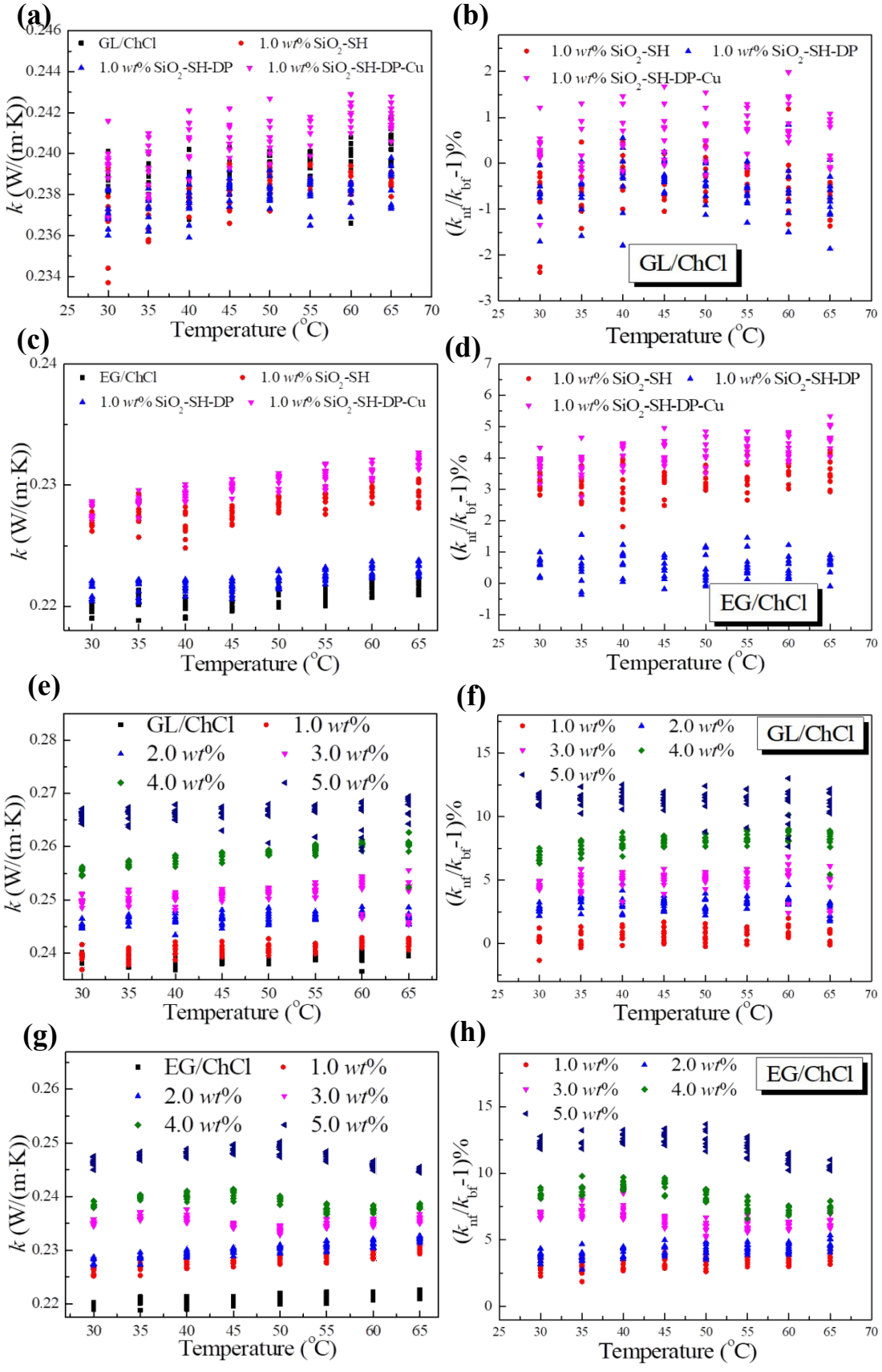

Fig. 5 Thermal conductivity (a) and thermal conductivity enhancement (b) of GL/ChCl based nanofluids with

different types of nanofillers; thermal conductivity (c) and thermal conductivity enhancement (d) of EG/ChCl based nanofluids with different types of nanofillers; thermal conductivity (e) and thermal conductivity enhancement (f) of GL/ChCl based nanofluids with different mass fraction of SiO_2-SH-DP-Cu; thermal conductivity (g) and thermal conductivity enhancement (h) of EG/ChCl based nanofluids with different mass fraction of SiO_2-SH-DP-Cu.

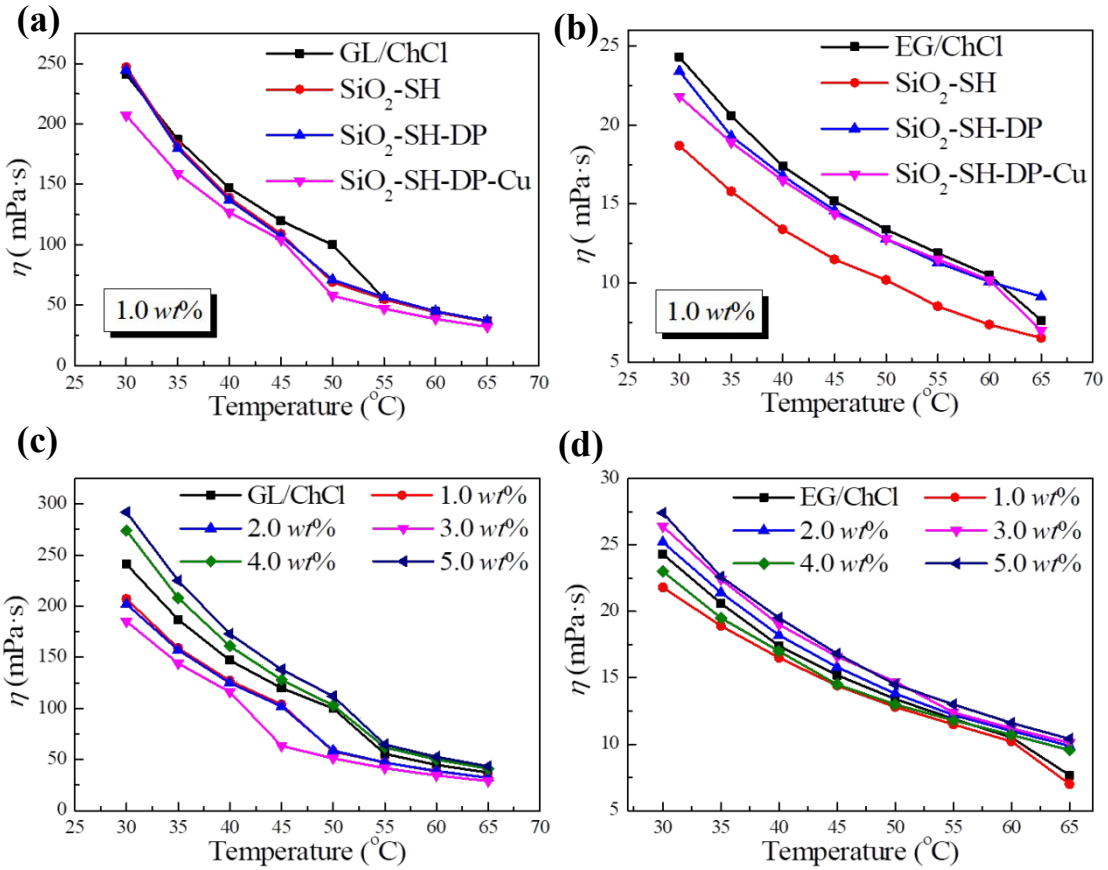

Fig. 6 Viscosity of (a) GL/ChCl and (b) EG/ChCl based nanofluids with different types of nanofillers; viscosity of (c) GL/ChCl and (d) EG/ChCl based nanofluids with different mass fraction of SiO_2-SH-DP-Cu.

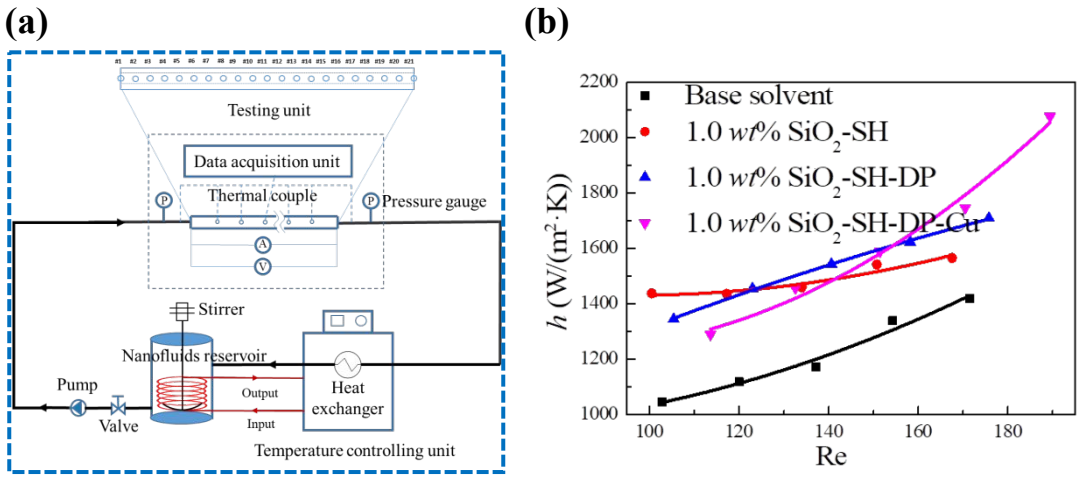

Fig. 7 (a) Schematic diagram of convective heat transfer coefficient testing platform, (b) convective heat transfer coefficient as a function of Reynolds number.

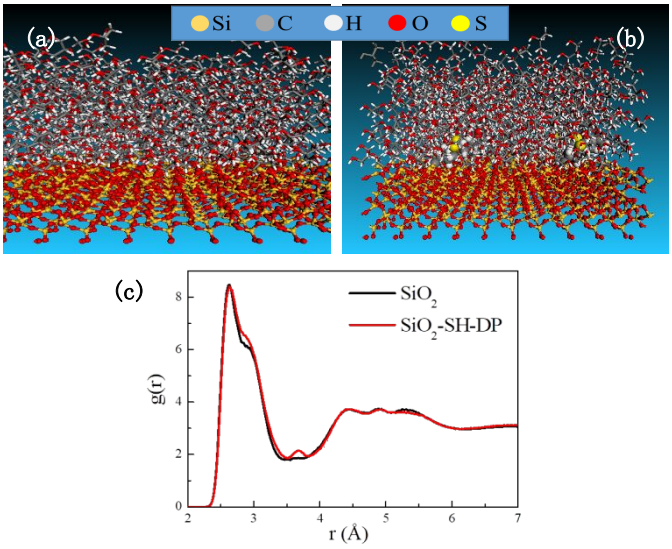

Fig. 8 Molecule model description of (a) SiO_2/glycerol system, (b) SiO_2-SH-DP/glycerol system, (c) the number of vicinal oxygen atom on the surface of nanoparticles as a function of radial distribution.

Table 1 Summary of silica nanoparticles in this work.

Sample name	Preparation procedure
SiO_2-SH	Made from TEOS and MPTMS through a base mediated sol-gel method
SiO_2-SH-DP	Treated SiO_2-SH with DP under the catalysis of Lewis acid
SiO_2-SH-DP-Cu	Treated SiO_2-SH-DP with $Cu(acac)_2$ and followed by $NaBH_4$ reduction

Table 2 Some reported results on the thermal conductivity performance of silica filled nanofluids.

Base solvent	Author	Fraction of silica	Thermal conductivity enhancement (%)	Reference
Water	Hwang et al.	1.0 *vol*%	3.0	[53]
Water	Iqbal et al.	1.0 *vol*%	6.0	[54]
Water	Yan et al.	5.0 *wt*%	6.8	[55]
Water	Xie et al.	4.0 *vol*%	10.0	[56]
Water	Pryazhnikov et al.	2.0 *vol*%	7.2	[57]
Water	Ferrouillat et al.	5.0 *wt*%	10.0	[58]
Ethanol	Mohammad et al.	0.44 *vol*%	6.0	[59]
GL	Akilu et al.	2.0 *vol*%	6.1	[60]
Water	Guo et al.	0.5 *vol*%	1.0	[61]
EG	Guo et al.	1.0 *vol*%	3.4	[61]

Table 3 Some related thermo-physical parameters of EG/ChCl based nanofluids.

Nanoparticle	Density (Kg/m^3)	Specific heat	Viscosity (mPa·s)

		capacity (J/(Kg·K))	
--	1086.4	2.504	24.2
SiO_2-SH	1083.5	2.503	24.7
SiO_2-SH-DP	1076.8	2.504	23.4
SiO_2-SH-DP-Cu	1081.0	2.504	21.8

Table 4 The diffusion coefficient and lifetime of SiO_2/glycerol heterogeneous system.

Heterogeneous system	Diffusion coefficient ($\times 10^{-12}$ $m^{-1}\cdot s^{-1}$)	Lifetime of hydrogen bond (fs)
SiO_2/Glycerol	3.32975	539.563
SiO_2-SH-DP/Glycerol	1.86119	541.798

For Table of Contents Use Only
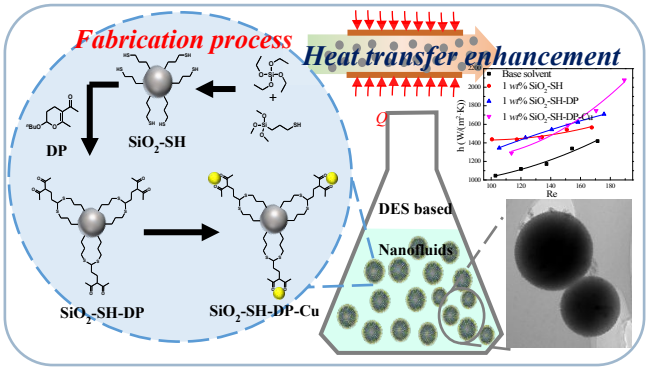
A chemically decorated silica filled DES based nanofluid that could fulfill both thermal conductivity enhancement and static stability was fabricated.